BJ www.biochemj.org

BJ Cell

Biochem. J. (2008) **415**, 345–351 (Printed in Great Britain) doi:10.1042/BJ20081411

online data multimedia

ACCELERATED PUBLICATION

Depletion of nucleophosmin leads to distortion of nucleolar and nuclear structures in HeLa cells

Mohammed Abdullahel AMIN, Sachihiro MATSUNAGA, Susumu UCHIYAMA and Kiichi FUKUI[1]

Department of Biotechnology, Graduate School of Engineering, Osaka University, 2-1 Yamadaoka, Suita 565-0871, Osaka, Japan

NPM (nucleophosmin; also known as B23) is an abundantly and ubiquitously expressed multifunctional nucleolar phosphoprotein, which is involved in numerous cellular processes, including ribosome biogenesis, protein chaperoning and centrosome duplication; however, the role of NPM in the cell cycle still remains unknown. In the present study, we show dynamic localization of NPM throughout the cell cycle of HeLa cells. Using a combination of RNAi (RNA interference) and three-dimensional microscopy we show that NPM is localized at the chromosome periphery during mitosis. We also demonstrate that depletion of NPM causes distortion of nucleolar structure as expected and leads to unexpected dramatic changes in nuclear morphology with multiple micronuclei formation. The defect in nuclear shape of NPM-depleted cells, which is clearly observed by live-cell imaging, is due to the distortion of cytoskeletal (α-tubulin and β-actin) structure, resulting from the defects in centrosomal microtubule nucleation. These results indicate that NPM is an essential protein not only for the formation of normal nucleolar structure, but also for the maintenance of regular nuclear shape in HeLa cells.

Key words: HeLa cell, nuclear structure, nucleolar structure, nucleophosmin (NPM), RNA interference (RNAi).

INTRODUCTION

The most active and dynamic nuclear domain, the nucleolus, plays a prominent role in the organization of various components of the nucleus and is considered as plurifunctional [1]. In addition to ribosome production, maturation and assembly [2], the nucleolus plays important roles in the regulation of numerous cellular processes, including cell-cycle regulation, apoptosis, telomerase production, RNA processing monitoring and response to cellular stress [3–5]. NPM (nucleophosmin), a major nucleolar protein continuously shuttles between the nucleus and cytoplasm [6]. NPM acts as an oncogene and is required for the development of the mouse embryo [7,8]. Other reports have shown that NPM acts as a tumour supressor [9,10]. Thus the role of NPM in oncogenesis still remains controversial. Moreover, its roles in the structure of the nucleolus and nucleus are still unknown.

It is reasonable that depletion of nuclear or related proteins causes abnormal nuclear morphology [11,12]. Interestingly, depletion of nucleolar protein fibrillarin also showed aberrant nuclear morphology and growth inhibition [13]. Thus the nucleolus has been reported to function in cell survival and to contribute in the general nuclear function and architecture [14].

In the present study, we show that NPM is dynamically localized throughout the cell cycle and interacts with other major nucleolar proteins, fibrillarin and nucleolin. Using RNAi (RNA interference), we demonstrate that NPM is localized at the chromosome periphery. We also demonstrate that depletion of NPM leads to distortion of nucleolar and nuclear structures with micronuclei formation. Moreover, NPM knockdown abolishes centrosomal microtubule nucleation, resulting in the distortion of cytoskeletal elements.

EXPERIMENTAL

Cell culture, siRNA (small interfering RNA) transfection and rescue assay

HeLa cells were cultured in DMEM (Dulbecco's modified Eagle's medium; Gibco BRL) supplemented with 5 % (v/v) FBS (fetal bovine serum) at 37 °C in a humidified incubator with 5 % CO_2. Cells were treated with 2.5 mM thymidine (Sigma) for 16 h, washed and released into fresh medium for 8 h, and then treated with thymidine for a further 16 h to obtain cells uniformly blocked at the G_1–S-phase boundary. At 12 h after release from the second thymidine block, cells were harvested for further analysis.

A double-stranded siRNA sequence (5′-AGAUGAUGAUGA-UGAUGAUTT-3′) was used to knockdown human NPM. An siRNA sequence specific for GL2 luciferase gene was used for control RNAi (mock) [13]. The siRNA sequences for fibrillarin and nucleolin have been published previously [13,15]. siRNA transfection was performed according to manufacturer's protocol (Invitrogen). For the siRNA rescue assay, we constructed an NPMr [RNAi-refractory GFP (green fluorescent protein)-NPM] vector by introducing three silent mutations into the vector through changing the nucleotide sequence (residues 671–682) of NPM to GACGATGACGAC (the underlined nucleotides indicate silent mutations). Site-directed mutagenesis was performed by PCR and confirmed by sequencing. The RNAi-refractory construct was transfected into 24-h-old HeLa cell cultures using FuGENE™ 6 (Roche) before ~6 h of siRNA transfection. At 24- and 48-h post-transfection, cells were harvested and used for further experiments.

Abbreviations used: DIC, differential interference contrast; FBS, fetal bovine serum; GFP, green fluorescent protein; NE, nuclear envelope; NPM, nucleophosmin; PNB, pre-nucleolar body; RNAi, RNA interference; NPMr, RNAi-refractory GFP-NPM; siRNA, small interfering RNA.

[1] To whom correspondence should be addressed (email kfukui@bio.eng.osaka-u.ac.jp).

© 2008 The Author(s)

The author(s) has paid for this article to be freely available under the terms of the Creative Commons Attribution Non-Commercial Licence (http://creativecommons.org/licenses/by-nc/2.5/) which permits unrestricted non-commerical use, distribution and reproduction in any medium, provided the original work is properly cited.

Biochemical Journal

Microtubule-polymerization assay

HeLa cells were transfected on to coverslips with mock or NPM siRNAs. At 48 h after transfection, cells were transferred to ice-cold medium supplemented with 10 mM Hepes (pH 7.25) for 30 min for the depolymerization of microtubules. Cells were then transferred to medium at 37 °C for 0, 30 and 60 s and 5 min so that microtubules could be allowed to re-grow and these were then fixed immediately in 99.8 % methanol at −20 °C.

Western-blot analysis

Western-blot analysis was performed using standard methods. The mouse monoclonals against B23/NPM (Santa Cruz Biotechnology), α-tubulin (Calbiochem) and β-actin (Sigma) were used at 1:500 to detect NPM, tubulin and β-actin respectively. Goat anti-(lamin A/C) (Santa Cruz Biotechnology) was used at 1:100 to detect lamin A/C, and mouse anti-nucleolin (Abcam) and rabbit anti-fibrillarin (Abcam) at 1:250 were used to detect nucleolin and fibrillarin respectively. Secondary antibodies conjugated to alkaline phosphatase (anti-mouse from Leinco Technologies; anti-rabbit and anti-goat from Vector Laboratories) were used for immunoreactions, which were finally detected by NBT (Nitro Blue Tetrazolium)/BCIP (5-bromo-4-chloroindol-3-yl phosphate) solution (Roche) in alkaline phosphatase buffer [100 mM Tris/HCl (pH 9.5), 100 mM NaCl and 1 mM $MgCl_2$].

Indirect immunofluorescence microscopy

HeLa cells grown on coverslips and fixed with 4 % (w/v) paraformaldehyde at 37 °C or 99.8 % methanol at −20 °C were incubated with primary antibodies. The antibodies used in the present study were as follows: goat anti-NPM and anti-(lamin A/C) at 1:50; mouse monoclonal antibodies against α-tubulin, β-actin, Ki-67 (Dako) and nucleolin at 1:100; mouse monoclonal antibody against NPM (Santa Cruz Biotechnology) at 1:1000; human anti-centromere autoantibody (CREST; Cortex Biochem) at 1:1000; and a rabbit polyclonal anti-fibrillarin antibody (Abcam) at 1:100. Immunofluorescence staining was performed using standard methods. DNA was stained with Hoechst 33342 (Sigma). All images were acquired as z-stacks with 0.2-μm spacing using a ×100, 1.3 NA oil objective on an IX-70 microscope (Olympus) and processed by iterative constrained deconvolution (SoftWorx, Applied Precision Instruments). Images were cropped, sized and arranged into panels using Adobe Photoshop CS version 8.0 (Adobe Systems).

Live-cell imaging

HeLa cells stably expressing GFP–histone H1.2 grown on 35-mm poly-L-lysine-coated glass-bottomed dishes (Matsunami) were transfected with siRNA sequences. The medium was changed to a CO_2-independent medium (Gibco BRL) supplemented with 10 % (v/v) FBS, 0.1 μg/ml penicillin/streptomycin, 20 mM glutamate and 100 mM Hepes before 1 h of imaging. The sequence of fluorescence images was acquired at every 6 min using a 40×, 1.4 NA oil objective on an inverted fluoresecence microscope (IX-81, Olympus) equipped with a z-motor and CCD (charge-coupled device) camera (Photometrics). Experiments were performed in a chamber maintained at 37 °C with a humidified atmosphere of 5 % CO_2 in air. Metamorph software (Universal Imaging) and the WCIF (Wright Cell Imaging Facility) ImageJ Program (http://www.uhnresearch.ca/facilities/wcif/fdownload.html) were used for acquisition and analysis.

RESULTS AND DISCUSSION

Previously, our proteomic analyses of highly purified human metaphase chromosomes showed that NPM was located at the chromosome periphery [16]. In the present study, we examined the localization of NPM throughout the cell cycle of fixed HeLa cells by double immunostaining. NPM is dynamically localized from interphase to telophase (Figure 1A). In interphase, NPM is mainly located in the dense fibrillar components and granular components of nucleoli, and also in the nucleoplasm as scattered foci. In prophase, NPM is dispersed due to nucleolar disintegration. In prometaphase, NPM moves towards the chromosome periphery where it remains until anaphase. The localization of NPM at the chromosome periphery was confirmed using an RNAi method. Chromosome-spread and immunostaining experiments showed that NPM signals were robust at the chromosome periphery of mock-treated cells, whereas those were absent in the case of NPM-depleted cells (Figure 1B). NPM is also distributed throughout the cytoplasm during mitosis. In telophase, NPM is concentrated into PNBs (pre-nucleolar bodies) and is involved in the eventual establishment of daughter nucleoli before NE (nuclear envelope) formation. Thus NPM actively shuttles from the nucleolus to perichromosomal region and cytoplasm only after NE breakdown at the end of prophase, and returns back to the PNBs and nucleoplasm at the end of telophase. These results indicate that NPM is a highly dynamic protein throughout the cell cycle.

In early G_1-phase cells, NPM is found to localize at the PNBs, nucleoplasm and inner nuclear membrane as scattered dots (Figure 1C). Previously, we showed that fibrillarin and nucleolin were also localized at the chromosomal periphery and in the PNBs [13,15]. Nucleolin interacts with fibrillarin [15], and NPM directly interacts with nucleolin [17]. Taken together, our results indicate that fibrillarin, nucleolin and NPM are co-localized at the chromosome periphery and PNBs where they interact with each other during the cell cycle.

To understand the functional importance of NPM in the nucleolus, endogenous NPM was specifically depleted by RNAi in HeLa cells. Depletion of NPM levels was revealed by both Western-blot analysis and immunostaining (Figures 2A–2C). DIC (differential interference contrast) imaging showed that mock-treated cells presented, at best, three large, spherical intranuclear masses corresponding to nucleoli (Figure 2D). In contrast, the nucleolar masses appeared distorted and fragmented in several small spots in NPM-depleted cells (Figure 2D). Moreover, immunofluorescence showed that nucleolar marker proteins, such as fibrillarin, nucleolin and Ki-67, were associated with nucleoli in mock-treated cells (Figures 2E–2G), whereas they were associated with remnants of the nucleolar compartment in NPM-depleted cells, exhibiting the disorganized pattern of the nucleolar structure with a relatively reduced size (Figures 2E–2G). Western-blot analysis showed that NPM depletion did not significantly affect the expression level of nucleolin and fibrillarin as compared with mock-treated cells (Figure 2B). Moreover, single depletion of nucleolin or fibrillarin did not show any effect on the localization of each other and of NPM (Supplementary Figure S1 at http://www.BiochemJ.org/bj/415/bj4150345add.htm). NPM depletion caused distortion of the nucleolar structure in other cell lines, such as HEK (human embryonic kidney)-293T and NHDF (normal human dermal fibroblast) cells (Supplementary Figure 2 at http://www.BiochemJ.org/bj/415/bj4150345add.htm). These results indicate that endogenous NPM generally plays a crucial role in the maintenance of the structural integrity of the nucleolus, with an exception in the case of U2OS cells [18].

NPM-depleted cells showed aberrant nuclear morphology with micronuclei formation at 48-h post-transfection (Figures 3A and 3B). Approx. 50 % of NPM-depleted cells had defective nuclear morphologies of various types, such as irregular, ruffled, lobulated morphologies, and more than 12 % of cells formed

© 2008 The Author(s)
The author(s) has paid for this article to be freely available under the terms of the Creative Commons Attribution Non-Commercial Licence (http://creativecommons.org/licenses/by-nc/2.5/) which permits unrestricted non-commerical use, distribution and reproduction in any medium, provided the original work is properly cited.

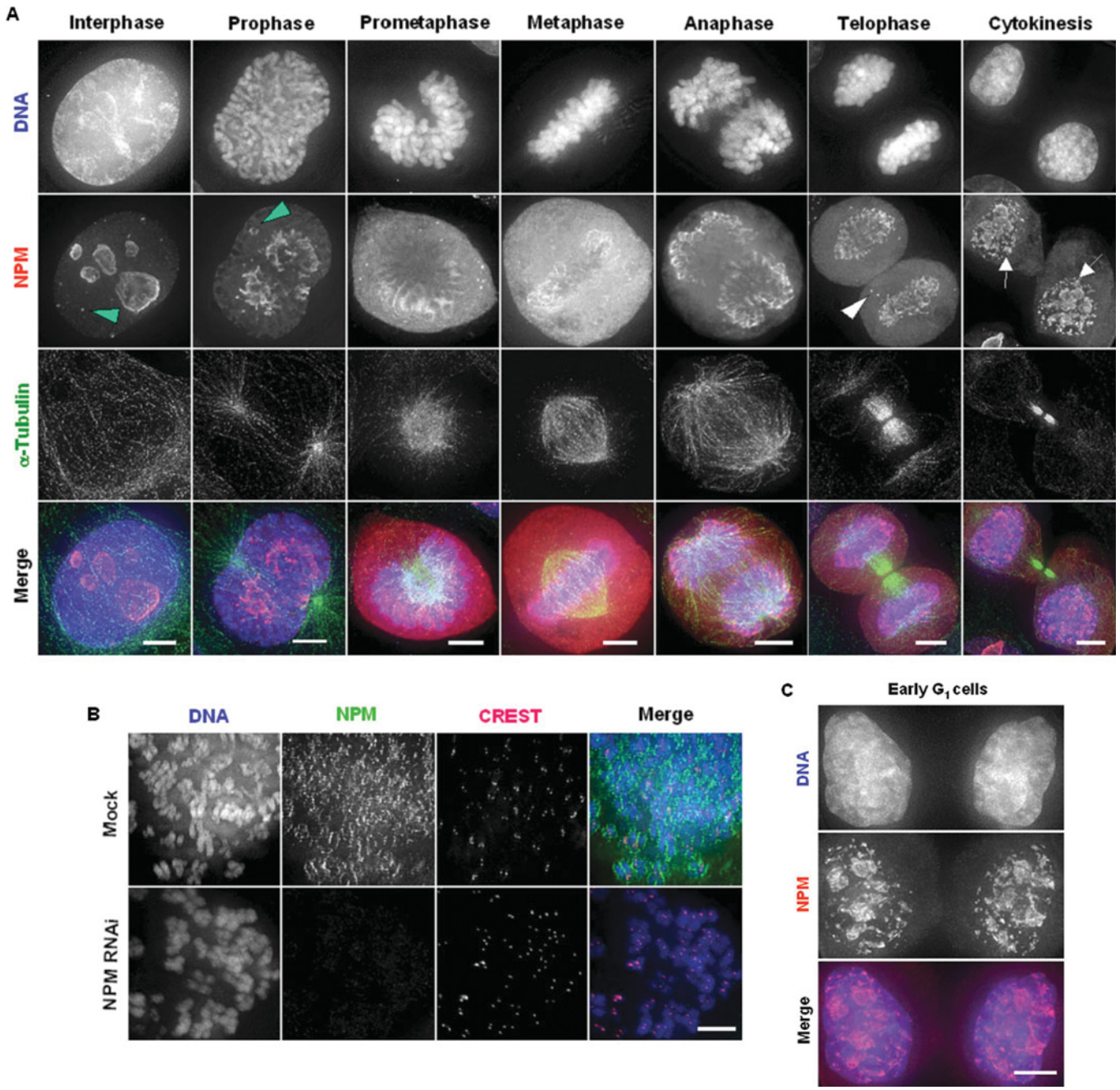

Figure 1 NPM is a highly dynamic protein and interacts with fibrillarin and nucleolin in the cell cycle

(**A**) HeLa cells fixed with paraformaldehyde were stained for NPM (red) and α-tubulin (green). DNA (blue) was counter-stained with Hoechst 33342. The green arrowheads indicate the foci of NPM at the nucleoplasm, the white arrowhead indicates the nucleolus-derived focus in the cytoplasm and white arrows indicate the PNBs in the newly forming nucleus. Scale bars, 5 μm. (**B**) Chromosome spread and immunostaining for NPM (green) and CREST (human anti-centromere autoantibody) (red) in mock and NPM RNAi cells. Scale bar, 5 μm. (**C**) Immunostaining of early G_1-phase cells for NPM (red) and DNA (blue). Scale bar, 5 μm.

multiple micronuclei (Figure 3C), whereas more than 98 % of mock-treated cells had the regular nuclear structure with almost no micronuclei formation. More than a 25- and 10-fold higher number of NPM-depleted cells had the aberrant nuclear morphology and multiple micronuclei respectively, compared with mock-treated cells. Obviously, the effect of NPM depletion at 48-h post-transfection on the nuclear structure is $\sim$2-fold higher than that of fibrillarin depletion (approx. 35 % of cells with nuclear defects at 72-h post-transfection [13]). These results indicate that NPM plays a more effective role on the nuclear morphology than fibrillarin. To rule out the potential off-target effects, we performed the rescue assay, which showed that these morphological changes were significantly recovered by introducing the NPMr plasmid (Figure 3C). An abnormal nuclear shape would develop from defects in mitosis or cytokinesis [19]. Moreover, down-regulation of NPM delays mitotic entry [20]. We then checked whether NPM depletion led or not to mitotic defects. Depletion of NPM caused accumulation of mitotic cells when HeLa cells were synchronously released from cell-cycle arrest at the G_1–S-phase boundary (Figure 3D). Moreover, at

© 2008 The Author(s)
The author(s) has paid for this article to be freely available under the terms of the Creative Commons Attribution Non-Commercial Licence (http://creativecommons.org/licenses/by-nc/2.5/) which permits unrestricted non-commerical use, distribution and reproduction in any medium, provided the original work is properly cited.

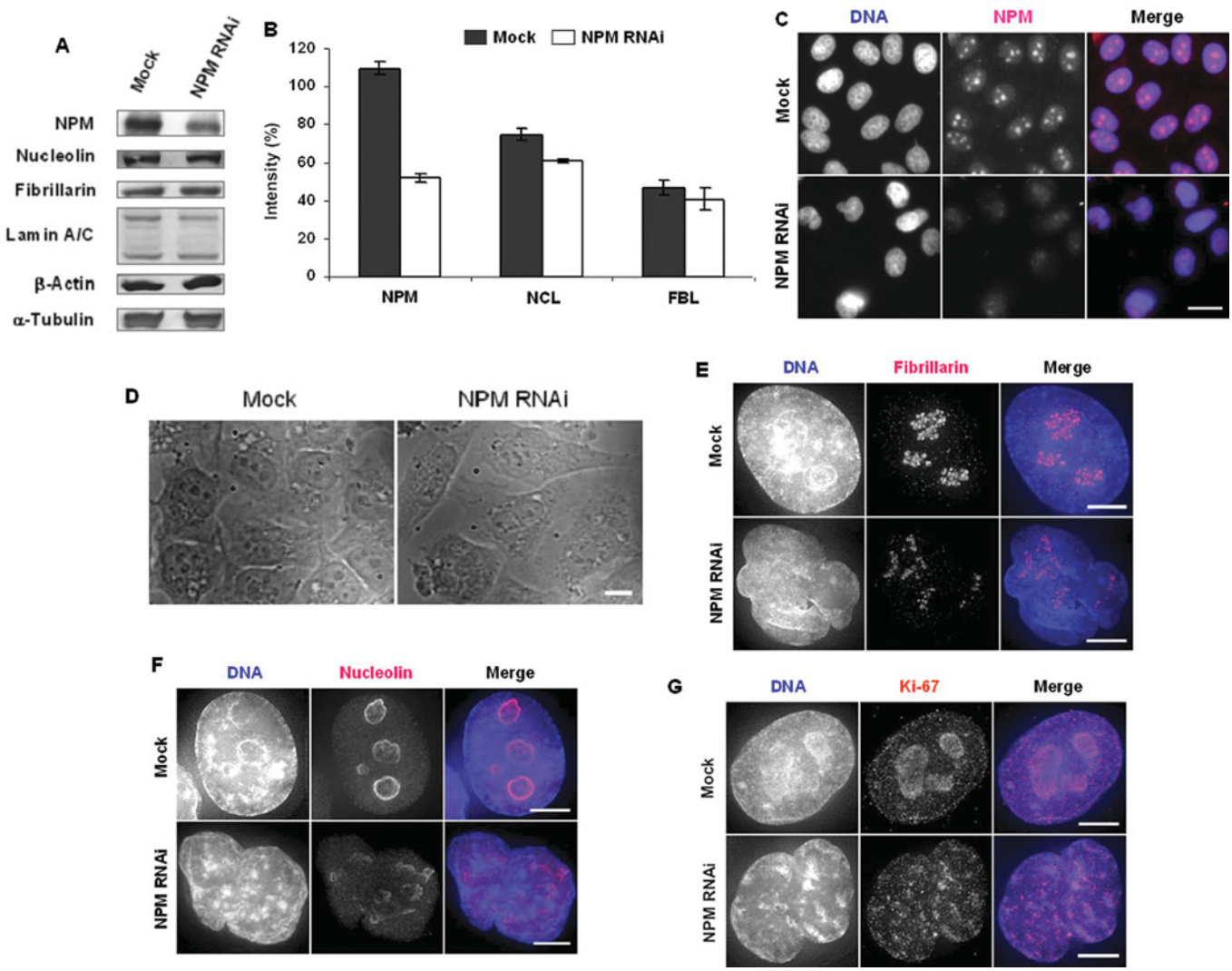

Figure 2 Depletion of NPM leads to a disorganized nucleolar structure in HeLa cells

(**A**) Western-blot analysis at 48-h post-transfection of mock and NPM RNAi cells. The NPM expression level was reduced to ~80% by RNAi. Other nucleolar proteins, such as fibrillarin and nucleolin, an NE protein, lamin A/C, and a cytoskeleton protein, β-actin, were immunoblotted. Western-blot analysis of α-tubulin served as loading controls. (**B**) Quantification of NPM, nucleolin (NCL) and fibrillarin levels in mock- and NPM-siRNA-treated cells in Western blots. Values are the means $\pm$ S.D. of three independent blots. (**C**) Immunostaining for NPM (red) and DNA (blue) in mock and NPM RNAi cells. Scale bar, 10 μm. (**D**) Phase-contrast images of fixed cells showing the pattern of nucleolar organization in mock-treated cells and the distortion of this pattern in NPM-depleted cells. Scale bar, 10 μm. (**E**–**G**) Immunostaining for nucleolar proteins in mock and NPM RNAi cells. (**E**) Fibrillarin (red), (**F**) nucleolin (red) and (**G**) Ki-67 (red); DNA is shown in blue. Scale bars, 5 μm.

24-h post-transfection of NPM-siRNA there was an accumulation of aberrant mitotic chromosomes in asynchronous cells, which were recovered by the rescue experiment (Figures 3E and 3F, and results not shown). Further transfection of NPM-siRNA until 48 h resulted in micronuclei formation at cytokinesis (Figure 3G). These results indicate that the defects in mitosis and/or cytokinesis in the absence of NPM would lead to the formation of an abnormal nuclear shape and micronuclei.

It is likely that irregular nuclear morphology may result from a defect in the post-mitotic assembly of the NE [21,22]; however, Western-blot analysis and immunofluorescence showed that the localization pattern and expression level of the NE protein, lamin A/C, were intact in NPM-depleted cells as well as in the mock-treated cells (Figures 2A and 4A). These results indicate that the nuclear defects in NPM-depleted cells were independent from the post-mitotic nuclear reassembly. Alternatively, nuclear abnormalities were reported to form independently from mitosis [12,13]. Live-cell imaging of HeLa GFP–histone H1.2 cells [23] clearly showed that approx. 50% of cells dramatically changed their nuclear morphology (Figure 4B and Supplementary Movies S1 and S2 at http://www.BiochemJ.org/bj/415/bj4150345add.htm). Cells not entering mitosis showed defects in the nuclear shape. These observations indicate that nuclear abnormality also occurs independently from mitosis. Thus nuclear shape defects in NPM-depleted cells are dependent and/or independent of mitosis.

Since nuclear morphology is strongly influenced by the cytoskeletal structure [24], the status of α-tubulin and β-actin was examined by immunofluorescence and Western-blot analysis. More than 66% of NPM-depleted cells had defects in the cytoskeletal structure (α-tubulin and β-actin elements became shrunken; Figures 4C and 4D), but the expression level of both cytoskeletal elements remained unaffected by NPM depletion compared with mock treatment (Figure 2A). The defects in cytoskeletal structure were remarkably recovered by

© 2008 The Author(s)
The author(s) has paid for this article to be freely available under the terms of the Creative Commons Attribution Non-Commercial Licence (http://creativecommons.org/licenses/by-nc/2.5/) which permits unrestricted non-commerical use, distribution and reproduction in any medium, provided the original work is properly cited.

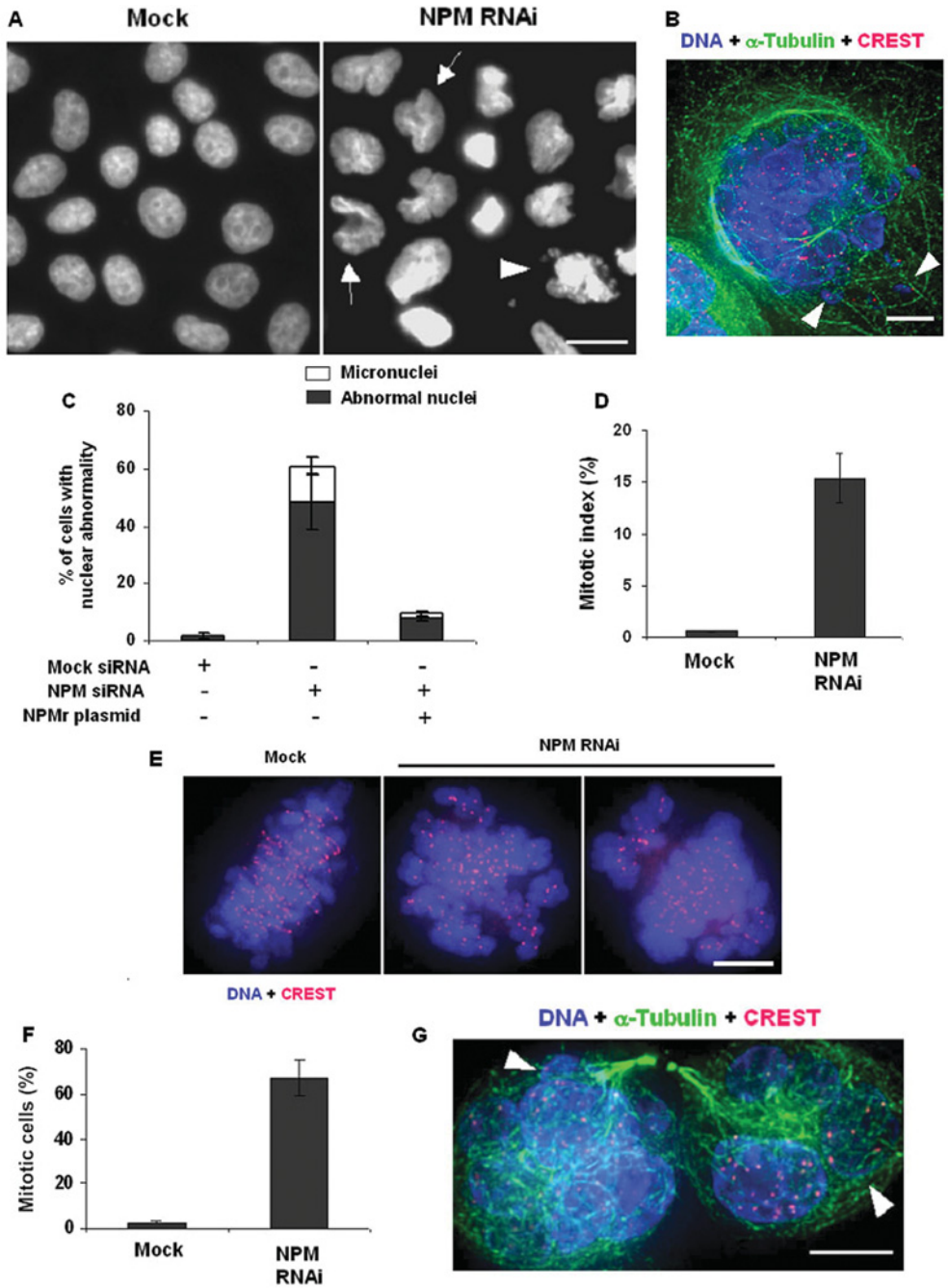

Figure 3 Depletion of NPM causes abnormal nuclear morphology and mitotic defects in HeLa cells

(**A**) Representative nuclear morphologies in mock (cells treated with control siRNA) and NPM RNAi cells. Arrows indicate cells with abnormal nuclear structure and the white arrowhead indicates micronucleated cells. Scale bar, 10 μm. (**B**) Cells containing micronuclei was stained with α-tubulin (green), CREST (human anti-centromere autoantibody) (red) and DNA (blue). Scale bar, 5 μm. The arrowheads indicate the micronuclei. (**C**) The percentage of cells showing irregular nuclear morphology and micronuclei formation and rescue of the defects in the presence of an NPMr plasmid. For both mock and NPM RNAi experiments, at least 400 cells were counted. Values are the means $\pm$ S.D. of at least triplicate cell counts ($P < 0.05$). (**D**) HeLa cells were synchronized at the G_1–S-phase boundary by a double-thymidine arrest, released into fresh medium and fixed at 12 h. The mitotic index was counted for both mock and NPM RNAi cells by immunostaining with α-tubulin and DNA. Values are the means $\pm$ S.D. of at least triplicate cell counts ($n = 800$–1000). (**E**) Aberrant chromosomes in asynchronous NPM-depleted cells. Scale bar, 5 μm. (**F**) The percentage of aberrant chromosomes in both mock and NPM RNAi cells. Values are the means $\pm$ S.D. of at least triplicate cell counts ($n = 100$). (**G**) An NPM-depleted cell forming micronuclei at cytokinesis at 48-h post-transfection was stained for α-tubulin (green), CREST (red) and DNA (blue). Scale bar, 5 μm. The arrowheads indicate the micronuclei.

the rescue experiments (Figure 4D). Although treatment with the microtubule-modifying agent nocodazole did not affect nuclear morphology in a way similar to NPM depletion (results not shown), we observed a marked defect in centrosomal microtubule re-polymerization after recovery from cold treatment in NPM-depleted cells (Figure 4E). Taken together, these observations indicate that aberrant nuclear morphology induced by NPM depletion is due to defects in microtubule polymerization and thus in cytoskeletal structure.

In summary, in the present study we explore the functional importance of NPM in the structural integrity of the nucleolus and nucleus in HeLa cells. We observed that depletion of NPM, rather

© 2008 The Author(s)
The author(s) has paid for this article to be freely available under the terms of the Creative Commons Attribution Non-Commercial Licence (http://creativecommons.org/licenses/by-nc/2.5/) which permits unrestricted non-commerical use, distribution and reproduction in any medium, provided the original work is properly cited.

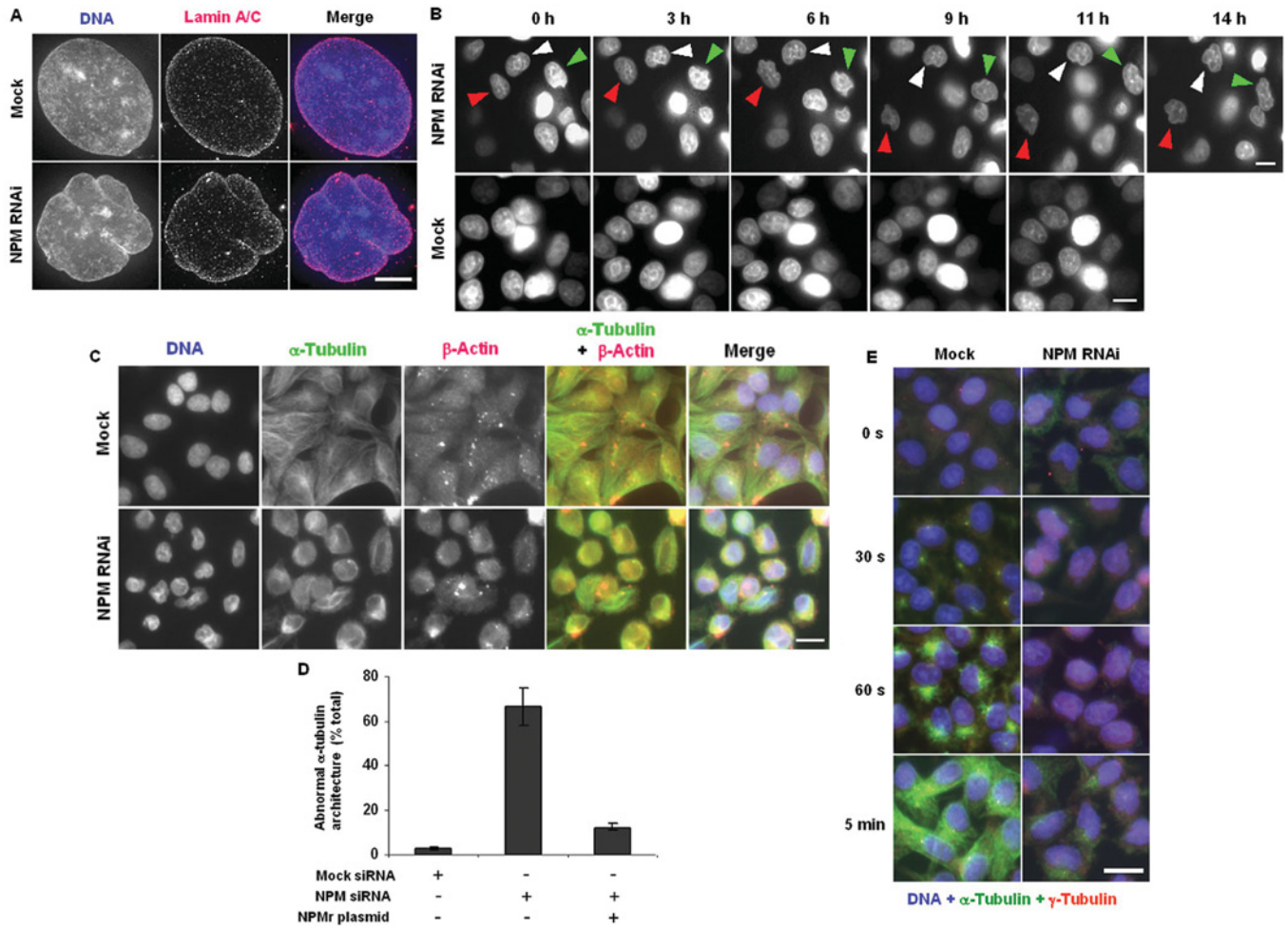

Figure 4 Defective nuclear structure in NPM-depleted cells is due to defects in microtubule polymerization and cytoskeletal structure in HeLa cells

(**A**) Mock and NPM RNAi cells were immunostained for lamin A/C (red) and DNA (blue). Scale bar, 5 μm. (**B**) Live-cell imaging of HeLa cells stably expressing GFP–histone H1.2. Cells were treated with NPM (top panels) and mock (lower panels) siRNAs for 21 h and then imaged at 6-min intervals for an additional 10–14 h. Representative photographs for both mock and NPM RNAi cells are shown. Cells indicated by green, red and white arrowheads in the top panels dramatically change their nuclear shape with time. Scale bar, 10 μm. (**C**) Mock and NPM RNAi cells were stained for α-tubulin (green), β-actin (red) and DNA (blue). Scale bar, 10 μm. (**D**) The percentage of cells showing a shrinked cytoskeletal structure. The defect in the tubulin skeleton is recovered in the presence of the NPMr plasmid. Values are the means $\pm$ S.D. of at least triplicate cell counts ($n =$ at least 300) ($P < 0.05$). (**E**) Re-polymerization of mock (left-hand panels) and NPM RNAi cells (right-hand panels). Cells were fixed and stained for γ-tubulin (red), microtubules (green) and DNA (blue) at 0, 30, 60 s and 5 min after recovery from cold treatment. Scale bar, 10 μm.

than nucleolin or fibrillarin, results in disorganized localization of the major nucleolar proteins. Although NPM, nucleolin and fibrillarin interact with each other during the cell cycle, among them only NPM would play a crucial role in maintaining the nucleolar integrity by keeping nucleolar proteins compact at the nucleoli. Moreover, we observed that cells have an aberrant nuclear structure in the absence of NPM. Although the exact reason why fibrillarin depletion causes abnormal nuclear shape is still unknown, NPM depletion leads to defective centrosomal microtubule nucleation and cytoskeletal structure, which may result in aberrant nuclear shape. Thus NPM would maintain the normal nuclear structure by maintaining the cytoskeletal structure through tubulin/actin fibres. From the results of the present study, we conclude that NPM is essential for the formation and structural integrity of the nucleolus and also for the maintenance of normal nuclear structure. These novel functions would further support the hypothesis that NPM is a multifunctional protein. NPM can bind nucleic acids [25] and appears to be involved in different aspects of DNA metabolism and chromatin regulation [26]. Although the exact mechanism of how NPM maintains nuclear structure is unknown, we speculate that the interactions of NPM with either chromatin/DNA or with the inner membrane in early G_1-phase are involved in providing the structural basis for a normal shaped nucleus. Moreover DIC imaging showed that cells with distorted nuclear shape also had distorted cellular structure (Supplementary Figure S3 at http://www.BiochemJ.org/bj/415/bj4150345add.htm), suggesting that cells with aberrant nuclear morphology eventually underwent apoptosis. Studies into the mechanism of how the changes in nuclear and cytoskeletal structures are connected with apoptosis will be important to understand the carcinogenic role of NPM.

We thank Dr Xin Wei Wang [Liver Carcinogenesis Section, Laboratory of Human Carcinogenesis, Center for Cancer Research, NCI (National Cancer Institute), NIH (National Institutes of Health), Bethesda, MD 20892, U.S.A.] for the GFP-tagged NPM vector. M. A. A. thanks the Ministry of Education, Culture, Sports, Science and Technology, Japan, and the International Graduate Program for Frontier Biotechnology, Graduate School of Engineering, Osaka University, for scholarship support. This work was supported by Special Co-ordination Funds of the Ministry of Education, Culture Sports, Sciences and Technology of the Japanese Government to K. F. and by Grants-in-Aid for Scientific Research from the Ministry of Education, Science, Culture, Sports, Science and Technology of Japan to K. F. and S. M.

© 2008 The Author(s)
The author(s) has paid for this article to be freely available under the terms of the Creative Commons Attribution Non-Commercial Licence (http://creativecommons.org/licenses/by-nc/2.5/) which permits unrestricted non-commerical use, distribution and reproduction in any medium, provided the original work is properly cited.

REFERENCES

1 Pederson, T. (1998) The plurifunctional nucleolus. Nucleic Acids Res. **26**, 3871–3876
2 Hadjiolov, A. A. (1985) The nucleolus and ribosome biogenesis. In Cell Biology Monographs (Alfert, M., Bergman, W., Goldstein, L., Porter, K. R. and Site, P., eds), pp. 1–268, Springer-Verlag Wien, New York
3 Olson, M. O. and Dundr, M. (2005) The moving parts of the nucleolus. Histochem. Cell Biol. **123**, 203–216
4 Lo, S. J., Lee, C. C. and Lai, H. J. (2006) The nucleolus: reviewing oldies to have new understandings. Cell Res. **16**, 530–538
5 Mayer, C. and Grummt, I. (2005) Cellular stress and nucleolar function. Cell Cycle **4**, 1036–1038
6 Borer, R. A., Lehner, C. F., Eppenberger, H. M. and Nigg, E. A. (1989) Major nucleolar proteins shuttle between nucleus and cytoplasm. Cell **56**, 379–390
7 Grisendi, S., Bernardi, R., Rossi, M., Cheng, K., Khandker, L., Manova, K. and Pandolfi, P. P. (2005) Role of nucleophosmin in embryonic development and tumorigenesis. Nature **437**, 147–153
8 Grisendi, S., Mecucci, C., Falini, B. and Pandolfi, P. P. (2006) Nucleophosmin and cancer. Nat. Rev. Cancer **6**, 493–505
9 Colombo, E., Bonetti, P., Denchi, E. L., Martinelli, P., Zamponi, R., Marine, J. C., Helin, K., Falini, B. and Pelicci, P. G. (2005) Nucleophosmin is required for DNA integrity and $p19^{Arf}$ protein stability. Mol. Cell. Biol. **25**, 8874–8886
10 Kurki, S., Peltonen, K., Latonen, L., Kiviharju, T. M., Ojala, P. M., Meek, D. and Laiho, M. (2004) Nucleolar protein NPM interacts with HDM2 and protects tumor suppressor protein p53 from HDM2-mediated degradation. Cancer Cell **5**, 465–475
11 Kimura, T., Ito, C., Watanabe, S., Takahashi, T., Ikawa, M., Yomogida, K., Fujita, Y., Ikeuchi, M., Asada, N., Matsumiya, K. et al. (2003) Mouse germ cell-less as an essential component for nuclear integrity. Mol. Cell. Biol. **23**, 1304–1315
12 Ulbert, S., Antonin, W., Platani, M. and Mattaj, I. W. (2006) The inner nuclear membrane protein Lem2 is a critical for normal nuclear envelope morphology. FEBS Lett. **580**, 6435–6441
13 Amin, M. A., Matsunaga, S., Ma, N., Takata, H., Yokoyama, M., Uchiyama, S. and Fukui, K. (2007) Fibrillarin, a nucleolar protein, is required for normal nuclear morphology and cellular growth in HeLa cells. Biochem. Biophys. Res. Commun. **360**, 320–326
14 Hernandez-Verdun, D., Roussel, P. and Gebrane-Younes, J. (2002) Emerging concepts of nucleolar assembly. J. Cell Sci. **115**, 2265–2270
15 Ma, N., Matsunaga, S., Takata, H., Ono-Maniwa, R., Uchiyama, S. and Fukui, K. (2007) Nucleolin functions in nucleolus formation and chromosome congression. J. Cell Sci. **120**, 2091–2105
16 Uchiyama, S., Kobayashi, S., Takata, H., Ishihara, T., Hori, N., Higashi, T., Hayashihara, K., Sone, T., Higo, D., Nirasawa, T. et al. (2005) Proteome analysis of human metaphase chromosomes. J. Biol. Chem. **17**, 16994–17004
17 Liu, H. T. and Yung, B. Y. (1999) *In vivo* interaction of nucleophosmin/B23 and protein C23 during cell cycle progression in HeLa cells. Cancer Lett. **144**, 45–54
18 Korgaonkar, C., Hagen, J., Tompkins, V., Frazier, A. A., Allamargot, C., Quelle, F. W. and Quelle, D. E. (2005) Nucleophosmin (B23) targets ARF to nucleolin and inhibits its function. Mol. Cell. Biol. **25**, 1258–1271
19 Yang, D., Welm, A. and Bishop, J. M. (2004) Cell division and cell survival in the absence of surviving. Proc. Natl. Acad. Sci. U.S.A. **101**, 15100–15105
20 Jiang, P. S. and Yung, B. Y. M. (1999) Down-regulation of nucleophosmin/B23 mRNA delays the entry of cells into mitosis. Biochem. Biophys. Res. Commun. **257**, 865–870
21 Foisner, R. and Gerace, L. (1993) Integral membrane proteins of the nuclear envelope interact with lamins and chromosomes and binding is modulated by mitotic phosphorylation. Cell **73**, 1267–1279
22 Ulbert, S., Plantani, M., Boue, S. and Mattaj, I. W. (2006) Direct membrane protein–DNA interactions required early in nuclear envelope assembly. J. Cell Biol. **173**, 469–476
23 Higashi, T., Matsunaga, S., Isobe, K., Morimoto, A., Shimada, T., Kataoka, S., Watanabe, W., Uchiyama, S., Itoh, K. and Fukui, K. (2007) Histone H2A mobility is regulated by its tails and acetylation core histone tails. Biochem. Biophys. Res. Commun. **357**, 627–632
24 Olins, A. L. and Olins, D. E. (2004) Cytoskeletal influences on nuclear shape in granulocytic HL-60 cells. BMC Cell Biol. **5**, 30
25 Wang, D., Baumann, A., Szebini, A. and Olson, M. O. J. (1994) The nucleic acid binding activity of nucleolar protein B23.1 resides in its carboxyl-terminal end. J. Biol. Chem. **269**, 30994–30998
26 Frehlick, L. J., Eirin-Lopez, J. M. and Ausio, J. (2007) New insights into the nucleophosmin/nucleoplasmin family of nuclear chaperones. Bioessays **29**, 49–59

Received 11 July 2008/18 August 2008; accepted 27 August 2008
Published as BJ Immediate Publication 27 August 2008, doi:10.1042/BJ20081411

© 2008 The Author(s)
The author(s) has paid for this article to be freely available under the terms of the Creative Commons Attribution Non-Commercial Licence (http://creativecommons.org/licenses/by-nc/2.5/) which permits unrestricted non-commerical use, distribution and reproduction in any medium, provided the original work is properly cited.

Biochem. J. (2008) **415**, 345–351 (Printed in Great Britain) doi:10.1042/BJ20081411

online data

SUPPLEMENTARY ONLINE DATA

Depletion of nucleophosmin leads to distortion of nucleolar and nuclear structures in HeLa cells

Mohammed Abdullahel AMIN, Sachihiro MATSUNAGA, Susumu UCHIYAMA and Kiichi FUKUI[1]

Department of Biotechnology, Graduate School of Engineering, Osaka University, 2-1 Yamadaoka, Suita 565-0871, Osaka, Japan

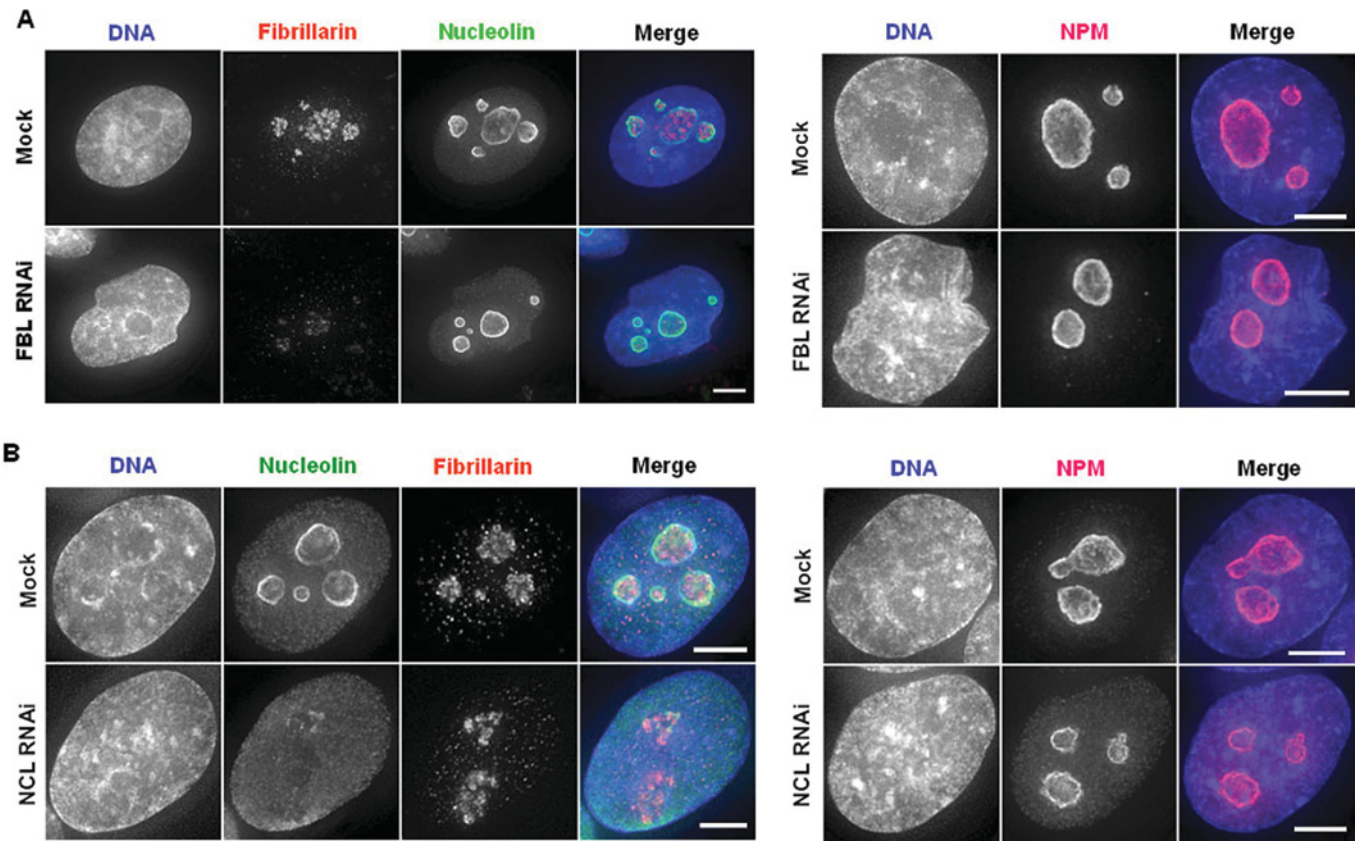

Figure S1 Depletion of nucleolin or fibrillarin does not affect the localization of nucleolar proteins

(**A**) Mock and fibrillarin (FBL) RNAi cells in interphase were stained for nucleolin (green) or fibrillarin (red) (left-hand panels) and NPM (red) (right-hand panels). DNA was counter-stained with Hoechst 33342 (blue). Scale bars, 5 μm. (**B**) Mock and nucleolin (NCL) RNAi cells in interphase were stained for nucleolin (green) or fibrillarin (red) (left-hand panels) and NPM (red) (right-hand panels). DNA was counter-stained with Hoechst 33342 (blue). Scale bar, 5 μm.

[1] To whom correspondence should be addressed (email kfukui@bio.eng.osaka-u.ac.jp).

© 2008 The Author(s)

The author(s) has paid for this article to be freely available under the terms of the Creative Commons Attribution Non-Commercial Licence (http://creativecommons.org/licenses/by-nc/2.5/) which permits unrestricted non-commerical use, distribution and reproduction in any medium, provided the original work is properly cited.

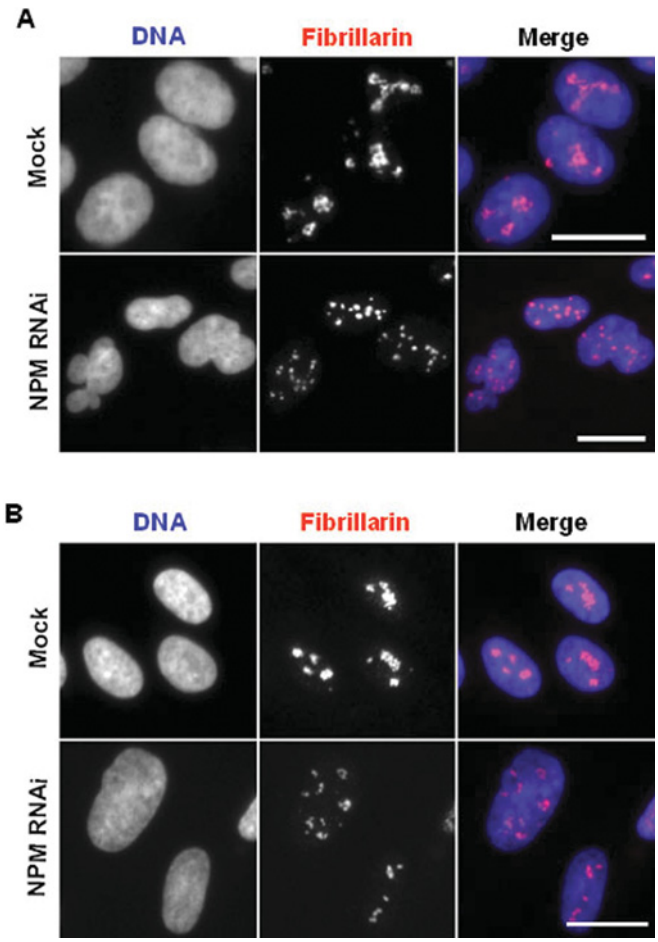

Figure S2 Depletion of NPM causes distortion of nucleolar structure in HEK (human embryonic kidney)-293T and NHDF (normal human dermal fibroblast) cell lines

Both mock and NPM RNAi cells were stained with fibrillarin (red) and DNA (blue) for HEK-293T (**A**) and NHDF cells (**B**). Scale bars, 10 μm.

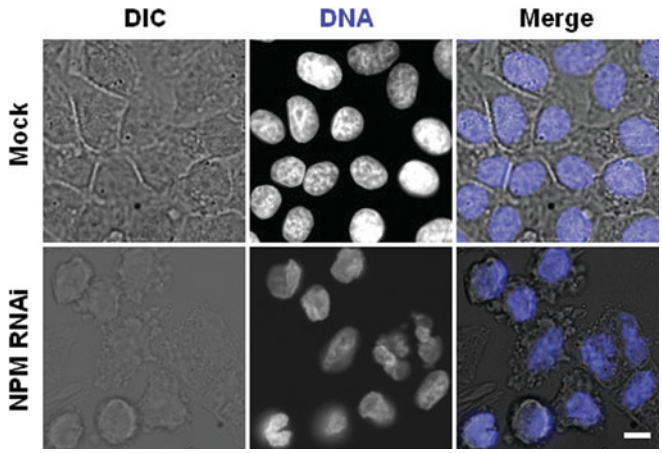

Figure S3 Image of cells under phase-contrast microscopy

The whole cellular structure is distorted by NPM depletion. Scale bar, 10 μm.

Received 11 July 2008/18 August 2008; accepted 27 August 2008
Published as BJ Immediate Publication 27 August 2008, doi:10.1042/BJ20081411

© 2008 The Author(s)
The author(s) has paid for this article to be freely available under the terms of the Creative Commons Attribution Non-Commercial Licence (http://creativecommons.org/licenses/by-nc/2.5/) which permits unrestricted non-commerical use, distribution and reproduction in any medium, provided the original work is properly cited.